

Synthesis of projection lithography for low k_1 via interferometry

Frank Cropanese^{*}, Anatoly Bourov, Yongfa Fan, Andrew Estroff, Lena Zavyalova, Bruce W. Smith
Center for Nanolithography Research, Rochester Institute of Technology, Rochester, New York

ABSTRACT

The aerial image attained from an optical projection photolithography system is ultimately limited by the frequency information present in the pupil plane of the objective lens. Careful examination of the frequency distribution will allow the operation of such a system to be synthesized experimentally through the use of interferometric lithography. Synthesis is accomplished through single beam attenuation in a two-beam interference system, which is equivalent to adjusting the relative intensities of the primary diffraction orders in a projection system. Typical lithography conditions, such as defocus and partial coherence, can be synthesized efficiently using this technique. The metric of contrast has been utilized to assess the level of correlation between defocus in a projection system and interferometric synthesis. Simulations have shown that interferometric lithography can approximate the performance of a variety of projection system configurations with a significantly high degree of accuracy.

Keywords: Interference, interferometric lithography, synthesis, single beam attenuation, defocus, contrast

1. INTRODUCTION

Fabrication of microelectronic devices requires increasingly smaller critical dimensions (CD). Extension of the utilization of optical lithography as the prevailing means of imaging these CD's requires the development of novel resolution enhancement technology (RET), such as high NA, phase-shift masking and partially coherent illumination. These techniques push resolution limits through k_1 optimization, which is the most cost effective method. Reduction of the process dependent factor k_1 is achieved through wavefront engineering by improving the spatial information of the object being imaged.

The spatial information in an optical system is represented by a complex amplitude consisting of magnitude and phase components. The magnitude and phase is characterized by the spatial distribution of the resultant electromagnetic field that is created upon diffraction at the reticle. Only a portion of the frequency information associated with the electromagnetic field is captured since the projection lens behaves as a low pass frequency filter. Typically, 1^{st} order frequencies (diffraction orders) must be collected in order to adequately reproduce the object at the image plane. The 0^{th} diffraction order is a zero frequency term that is generally incorporated to serve as a DC bias for the image intensity distribution created by higher frequencies.

Frequency analysis is of considerable concern when implementing some of the RET's that have been developed over recent years to address the need for k_1 optimization. The variety of mask configurations, illumination conditions and aberrations that exist in a conventional projection imaging system generate unique 0^{th} and 1^{st} diffraction orders that can have a significant impact on lithographic performance. The evaluation of different system configurations can be a cumbersome and costly task; however it is possible to synthesize the resulting behavior by utilizing a simple interferometric lithography system.

Interferometric lithography has been widely utilized in the analysis of newly developed photoresist chemistries and emerging lithographic techniques, such as immersion lithography. Interferometric lithography is accomplished through the interference of two mutually coherent light beams at the surface of a photosensitive substrate. The interfering beams generate a sinusoidal aerial image intensity distribution which consequently exposes a periodic pattern of lines and spaces in the substrate. The period (P) of this line and space array is a half-wavelength for numerical apertures

^{*} fcc8004@cis.rit.edu, Rochester Institute of Technology, 82 Lomb Memorial Dr., Rochester, NY 14623

($NA = \sin q$) approaching 1.0 and is given by the following equation, where λ is the exposing wavelength and q is the half-angle subtended by the two interfering beams:

$$P = \frac{\lambda}{2 \cdot NA} \quad (1)$$

Patterns exposed using interferometric lithography exhibit high contrast over a large depth of focus (DOF). The DOF is the latitude of an optical system to produce high resolution features in the presence of focal variation. Other advantages of interferometric lithography include the ability to be implemented inexpensively and with minimum complexity since there is limited use of masks and refractive components, which makes interferometric lithography well suited for research purposes.¹⁻³

2. THEORETICAL COMPARISON

A simple method for implementing the synthesis of projection lithography is through single beam attenuation in a two beam interference system. A single arm of the interferometer is blocked allowing additional exposure of the field with zero order intensity, or a DC bias. This zero order intensity has a demodulation affect on the aerial image that is comparable to the effect of “flare”. Flare is a phenomenon in projection optical systems where scattered and reflected light provide unwanted exposure to areas of the imaging field. Simulations were conducted to analyze the accuracy with which single beam attenuation approximates projection lithography by utilizing the fact that single beam attenuation is equivalent to increasing the level of flare in the system.

Projection conditions were simulated for various illumination conditions. Levels of defocus were applied to each of the projection systems, which resulted in a reduction of contrast of the intensity distribution. The intensity distribution was measured in an infinitely thick photoresist film with an assumed index of refraction of 1.60 and an absorption constant of $\alpha=0$. The exposed object consisted of a binary mask with 125nm 1:1 lines (pitch=250nm). The first projection configuration analyzed had a partial coherence of 0.5 sigma, an NA of 0.7, and defocus was varied from 0 to 80nm in steps of 10nm. The intensity distribution has been plotted in Figure 4 as a function of position. A two beam interference condition was created to synthesize the behavior of this system using a 0.5NA and additional single beam exposure intensity (flare) ranging from 7.4 to 46.9% of the original exposure intensity. The intensity in the resist film is plotted in Figure 5 after being renormalized to the mean intensity. A visual comparison of Figure 4 and Figure 5 demonstrate a significant degree of correspondence between the 0.5 sigma projection and the interference profiles. Additionally, the contrast curve in Figure 6 expresses that each curve, when plotted individually against defocus and flare, is identically matched to one another.

Analysis was also conducted for a projection configuration with a partial coherence of 0.7 sigma (0.6NA) and a setup with 0.85/0.55 (outer/inner) annular illumination (0.75NA). The intensity distribution in the resist for the 0.7 sigma and the annular systems is plotted in Figure 7 and Figure 10, respectively. In order to synthesize the 0.7 sigma partial coherence case defocus was varied from 0 to 80nm in steps of 10nm, which corresponded to flare values in the range of 7.3 to 28.2% of the original exposure when using interferometric lithography. The resulting intensity distribution, Figure 8, and the contrast curve comparison, Figure 9, demonstrate the excellent match between projection and interference synthesis, as with the 0.5 sigma system. Flare values in the range of 3.7 to 49.7%, Figure 11, were required in order to synthesize 0 to 240nm of defocus for the annular illumination condition. The contrast curve in Figure 12 displays the correlation between annular projection and interference.

3. EXPERIMENTAL IMPLEMENTATION

A Talbot interferometer was chosen to generate the two beam interference condition for this experiment. The two arms of the Talbot interferometer, for this specific case, are generated by passing a coherent light source through a fused silica phase grating. A 248nm KrF laser provided the illumination source and was passed through a beam expander, in order to expand the spatial coherence of the beam. The beam was then put through a polarizer so that the exposing illumination consists of only TE polarization, which maintains higher contrast at high NA's than TM polarization. The TE polarized light is deflected through the phase grating, which generates $\pm 1^{st}$ diffraction orders that are interfered at the photosensitive substrate surface utilizing two turning mirrors. Single beam attenuation is accomplished by blocking off

one of the arms of the interferometer and continuing to expose for a percentage of the original exposure time. The configuration used in this experiment is pictured in Figure 1.

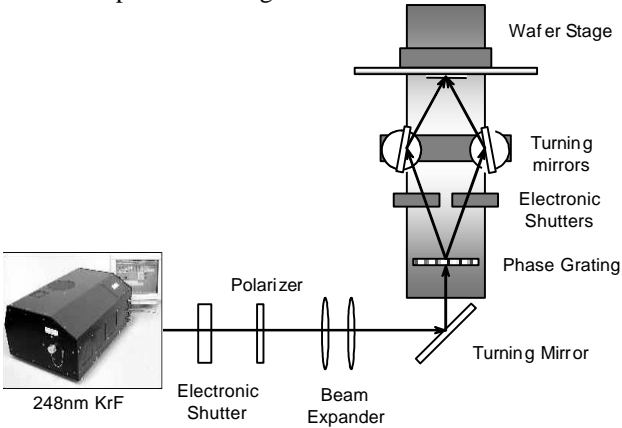


Figure 1 Experimental configuration for the implementation of interferometric lithography. The shutters on either end of the interferometer serve to accomplish single beam attenuation.

Interferometric lithography was performed with additional single beam exposure ranging from 0 to 90% of the original dose to size. The results for standard interferometric lithography, or 0% demodulation of the image intensity distribution, are pictured in Figure 2. The features maintain high contrast and there is minimal evidence of line edge roughness. Demodulation of the image intensity using 90% additional single beam exposure resulted in a visually noticeable reduction in contrast of the resist image. The features in Figure 3 display significant rounding of the tops of features as well as an increased degree of line edge roughness. A notable decrease in contrast was not found until the level of demodulation reached 90% due to the high contrast of the resist material utilized. A more accurate representation of the effect of demodulation on interference lithography may be obtained if a lower contrast photoresist material is used.

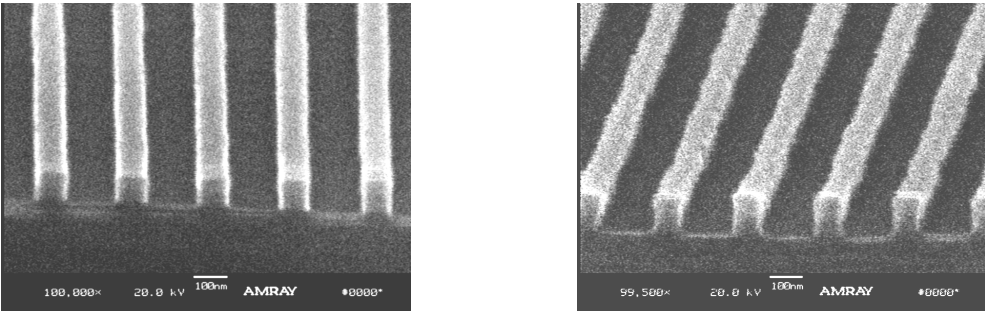


Figure 2 0.5NA Interferometric lithography with 0% additional exposure. The lines are of high contrast and there is minimal evidence of line edge roughness.

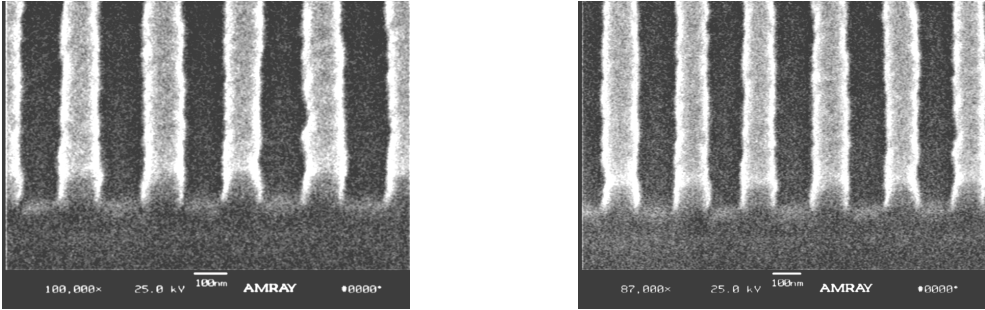


Figure 3 0.5NA Interferometric lithography with 90% additional exposure. There is a significant decrease in the image contrast and a high degree of line edge roughness.

4. CONCLUSIONS

Interferometric lithography, when coupled with intensity demodulation due to single beam attenuation, has been shown to be capable of synthesizing the effect of defocus on a variety of projection imaging configurations with an excellent degree of accuracy. The inexpensive nature and minimal complexity of this technique make it an attractive choice for the evaluation of emerging resist technologies and lithographic techniques, such as immersion, that would otherwise be cumbersome to reproduce experimentally. The introduction of the appropriate level of zero order intensity, or flare, is an effective method for emulating other aspects of lithography, i.e. partial coherence, phase shift masking and variable pitch.

5. REFERENCES

1. M. Switkes, T.M. Bloomstein and M. Rothschild, "Patterning of sub-50nm dense features with space-invariant 157nm interference lithography", *J. Vac. Sci. Technol.*, **B 19(6)**, 2353, 2001
2. W. Hinsberg, F.A. Houle, J. Hoffnagle, M. Sanchez, G. Wallraff, M. Morrison and S. Frank, "Deep-ultraviolet interferometric lithography as a tool for assessment of chemically amplified photoresist performance", *J. Vac. Sci. Technol.*, **B 16(6)**, 3689-3693, Nov/Dec 1998
3. J.A. Hoffnagle, W.D. Hinsberg, M. Sanchez and F.A. Houle, "Liquid immersion deep-ultraviolet interferometric lithography", *J. Vac. Sci. Technol.*, **B 17(6)**, Nov/Dec 1999
4. P.E. Dyer, R.J. Farley, R. Giedl, "Analysis and application of a 0/1 order Talbot interferometer for 193nm laser grating information", *Optics Communications*, **129**, 98-108, 1996

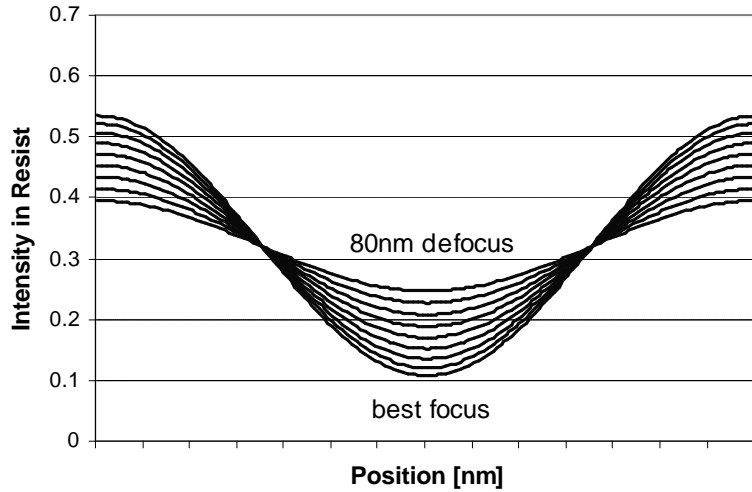


Figure 4

Intensity distribution in photoresist generated utilizing a projection configuration with a 0.5 sigma partial coherence, 0.7NA and a binary mask. Defocus was incremented from 0 to 80nm.

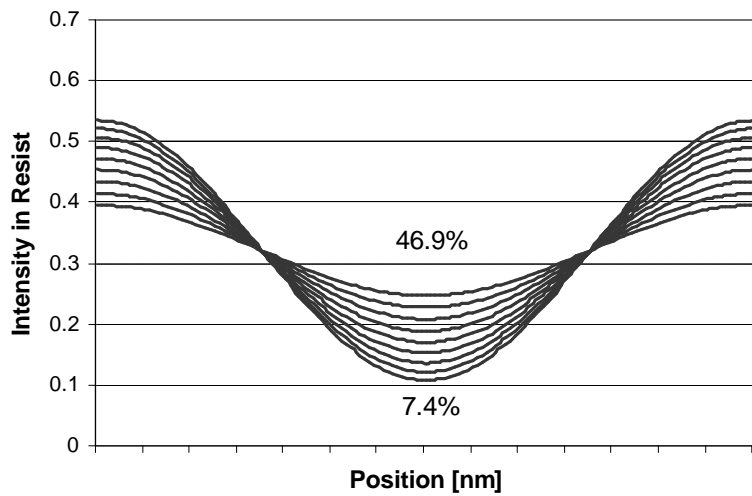


Figure 5

Intensity distribution in photoresist generated utilizing an interferometric configuration with a 0.5NA. Addition single beam exposure intensity ranged from 7.4 to 46.9% of the original dose.

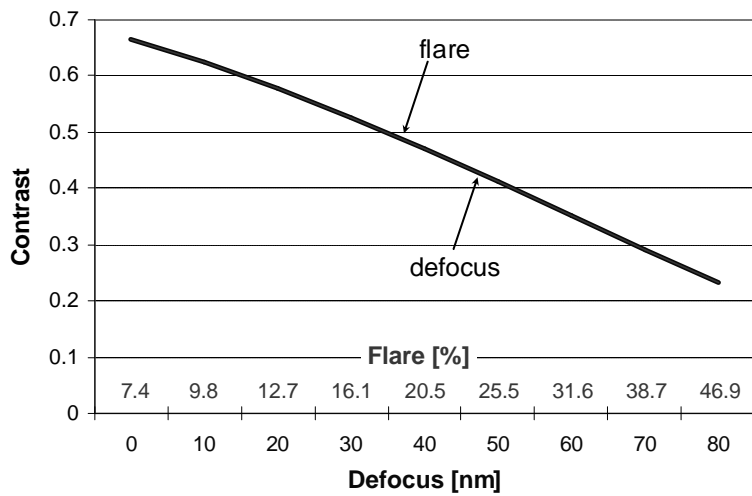


Figure 6

Correlation of additional single beam exposure (flare) in an interference system to defocus in a 0.5 sigma projection system. The trend in contrast for both systems is well matched.

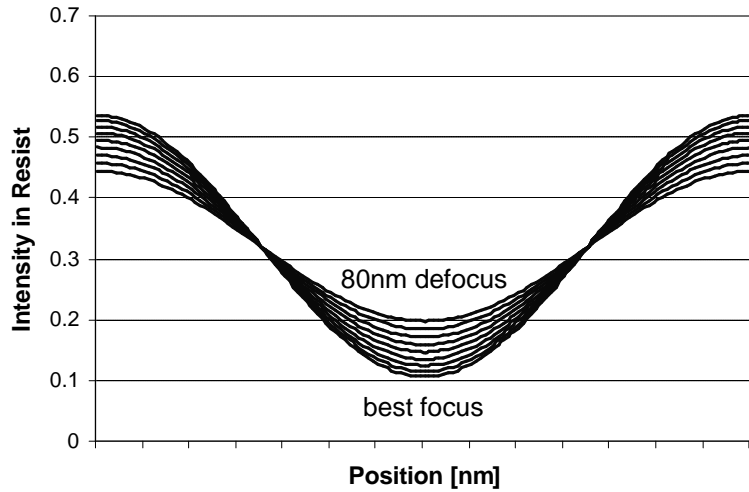


Figure 7

Intensity distribution in photoresist generated utilizing a projection configuration with a 0.7 sigma partial coherence, 0.6NA and a binary mask. Defocus was incremented from 0 to 80nm.

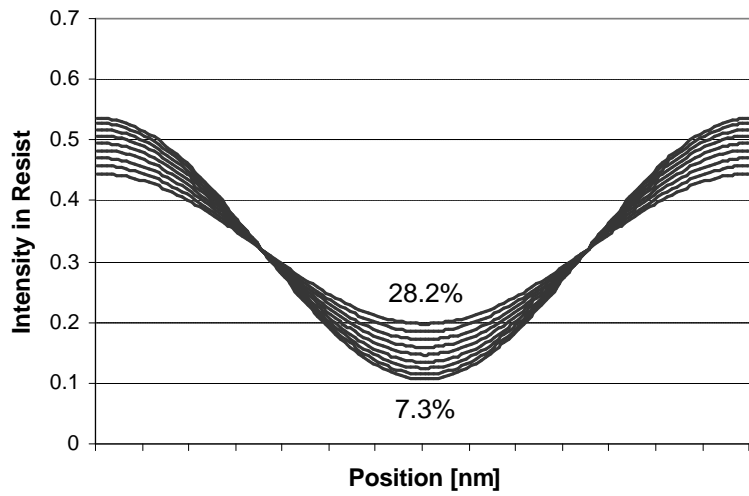


Figure 8

Intensity distribution in photoresist generated utilizing an interferometric configuration with a 0.5NA. Addition single beam exposure intensity ranged from 7.3 to 28.2% of the original dose.

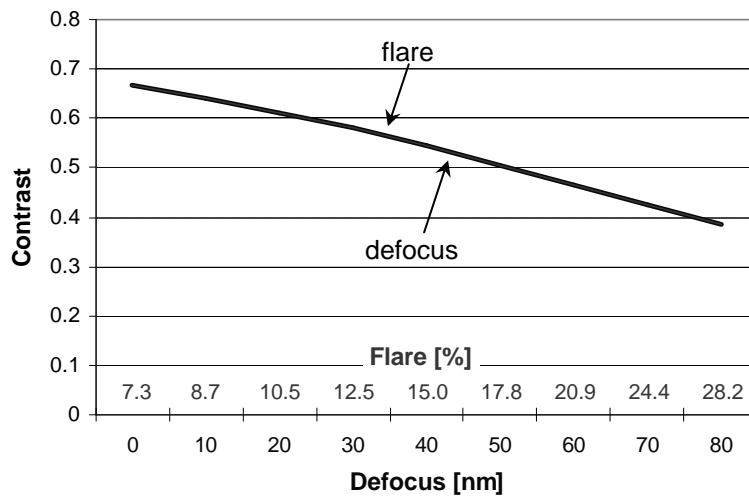


Figure 9

Correlation of additional single beam exposure (flare) in an interference system to defocus in a 0.7 sigma projection system. The trend in contrast for both systems is well matched.

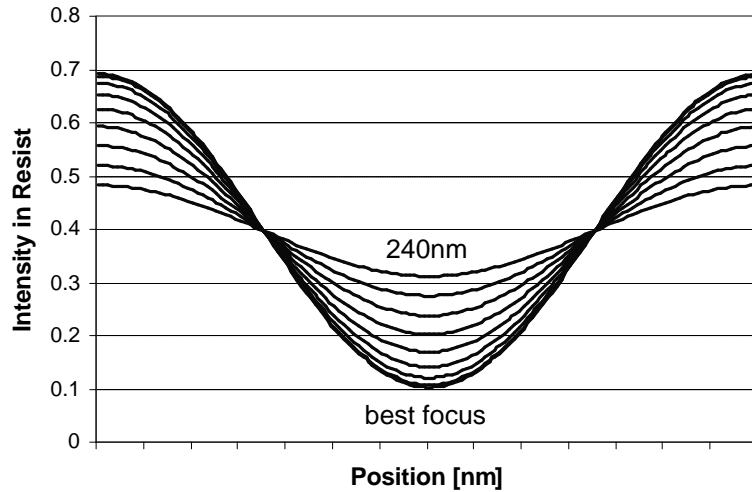


Figure 10

Intensity distribution in photoresist generated utilizing a projection configuration with annular illumination (0.85/0.55), 0.75NA and a binary mask. Defocus was incremented from 0 to 80nm.

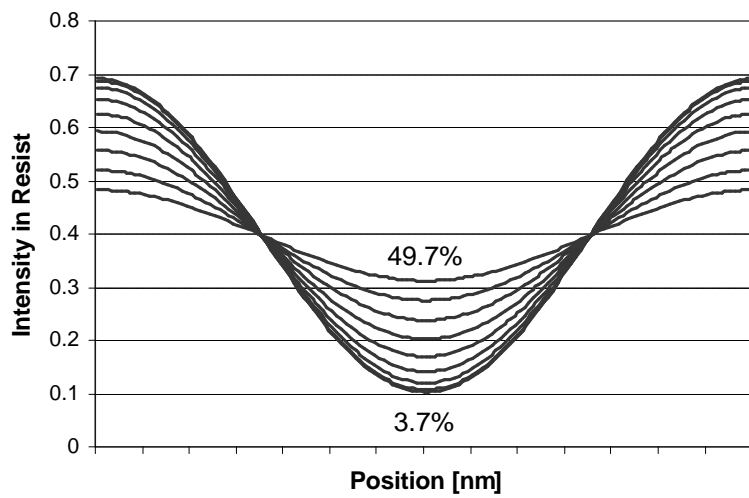


Figure 11

Intensity distribution in photoresist generated utilizing an interferometric configuration with a 0.5NA. Addition single beam exposure intensity ranged from 3.7 to 49.7% of the original dose.

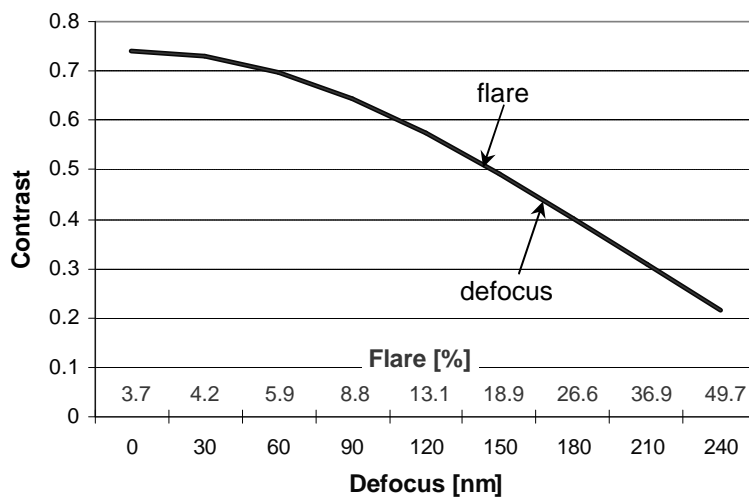


Figure 12

Correlation of additional single beam exposure (flare) in an interference system to defocus in annular (0.85/0.55) projection system. The trend in contrast for both systems is well matched.